Earth and Planetary Science Letters 475 (2017) 34–43

Contents lists available at ScienceDirect

Earth and Planetary Science Letters

www.elsevier.com/locate/epsl

Geometric disequilibrium of river basins produces long-lived transient landscapes

Helen W. Beeson [a,*,1], Scott W. McCoy [a], Amanda Keen-Zebert [b,2]

[a] Department of Geological Sciences and Engineering, Global Water Center, University of Nevada at Reno, United States
[b] Division of Earth and Ecosystem Sciences, Desert Research Institute, United States

ARTICLE INFO

Article history:
Received 8 March 2017
Received in revised form 29 June 2017
Accepted 4 July 2017
Available online xxxx
Editor: A. Yin

Keywords:
river basin dynamics
river reorganization
steady state
elevated low-relief surfaces
cratonic landscapes
erosion rate

ABSTRACT

Although equilibrium has long been considered the attractor state for landscapes, the time required to reach equilibrium or even the possibility of reaching equilibrium is still debated. Using ^{10}Be-based catchment-averaged denudation rates, topographic analysis, and analysis of the basin topology and geometry, including its area-channel length scaling relationship, we show that an ancient postorogenic dome on the North American Craton, the Ozark dome, is not in a state of equilibrium. The persistent state of disequilibrium on the Ozark dome is characterized by nonuniform erosion rates that vary by a factor of three, asymmetric drainage divides, and evidence for drainage rearrangement via stream capture. We find that planform geometric disequilibrium of river basins and drainage area exchange between adjoining basins can hold river networks in a disequilibrium state for potentially hundreds of million years and that, when sustained over time, erosion rate differences associated with drainage area exchange can lead to transient events such as stream capture and production of relief in the form of elevated, low-relief surfaces. Our results suggest that landscapes with slowly moving drainage divides might not reach equilibrium, and that river basin dynamics may contribute to setting the large-scale morphology of old cratonic landscapes.

1. Introduction

Owing largely to the manner in which erosion rates increase with increasing topographic gradient and relief (Ahnert, 1970; DiBiase et al., 2010), landscapes naturally evolve towards steady equilibrium forms in which rock uplift is balanced by erosion. The concept of steady state or equilibrium landscapes as time invariant forms has been central to the development, parameterization, and testing of geomorphic transport laws (Dietrich et al., 2003; Kirkby, 1971) and to interpretations of transient landscapes based on deviations from equilibrium forms (Kirby and Whipple, 2012; Tucker and Whipple, 2002; Whipple and Tucker, 1999). The possibility of reaching equilibrium depends on the response time of a landscape to changes in boundary conditions (Howard, 1982; Whipple, 2001). The time required to reach steady state after a tectonic or climatic perturbation is commonly equated to the timescale for individual basins to adjust river steepness such that rates of erosion and rock uplift are equal, which for many landscapes is thought to be on the order of millions of years (Pazzaglia, 2003; Whipple, 2001; Whipple and Tucker, 1999).

Field observations (Prince et al., 2011), analog experiments (Hasbargen and Paola, 2000; Reinhardt and Ellis, 2015), numerical modeling (Goren et al., 2014), and theory (Willett et al., 2014) demonstrates that planform basin shape and network topology can continue to adjust via divide migration and stream capture long after any perturbation to boundary conditions, which suggests that adjustments to basin geometry (Willett et al., 2014) may prolong landscape response times. If landscape response times are substantially prolonged by changing basin geometry, then transient landscapes may be more common and long-lived than previously thought, relief may be produced in the form of elevated, low-relief surfaces as nonuniform erosion rates persist, and the assumption that steady state conditions are achievable in all landscapes might be invalid. To test the hypothesis that river basin dynamics can protract time to steady state, we map and interpret disequilibrium in river basins draining the Paleozoic-aged Ozark dome. We show that aspects of the morphology of the Ozark dome reflect persistent river basin dynamics and that, although many fluvial lon-

* Corresponding author.
E-mail addresses: hbeeson@nevada.unr.edu, hwbeeson@gmail.com (H.W. Beeson), scottmccoy@unr.edu (S.W. McCoy), Amanda.Keen-Zebert@dri.edu (A. Keen-Zebert).
[1] University of Nevada, Department of Geological Sciences and Engineering, 1664 N. Virginia, MS 0172 Reno, NV 89557, United States.
[2] Desert Research Institute, 2215 Raggio Pkwy, Reno, NV 89512, United States.

http://dx.doi.org/10.1016/j.epsl.2017.07.010
0012-821X/

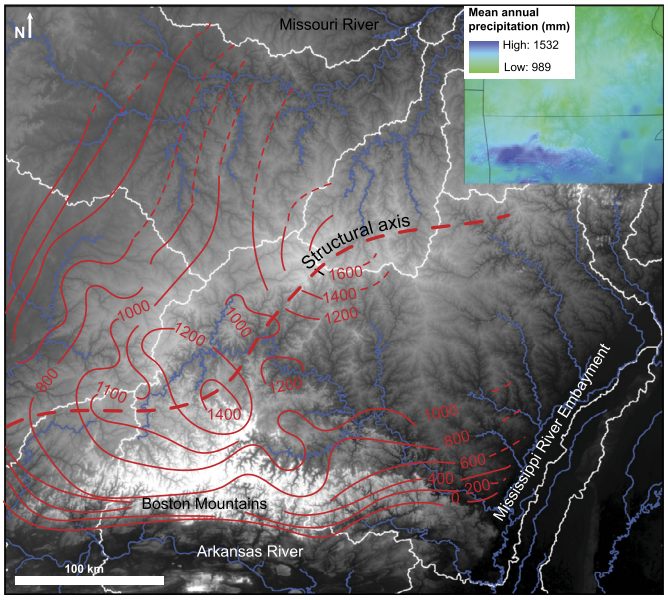

Fig. 1. Map of the Ozark dome. Hillshade of 90 m digital elevation model produced from the Shuttle Radar Topography Mission; white lines show major drainage divides, blue lines show major rivers, and red contours show structure contours mapping the base of the Mississippian limestone adapted from Siebenthal (1915). Inset shows mean annual precipitation (MAP) on the Ozark dome. Colors represent MAP based on 30-year normal data for 1981–2010 downloaded from PRISM Climate Group (http://prism.oregonstate.edu/normals/). (For a color version of this figure, the reader is referred to the web version of this article.)

gitudinal profiles on the Ozark dome have shapes approximating equilibrium forms, the fluvial network as a whole will likely never achieve steady state conditions owing to the disparity in timescales between geometric adjustment in landscapes with slowly moving drainage divides and comparatively rapid fluvial response times.

2. Testing for equilibrium and drainage divide motion in a tectonically-stable cratonic landscape

The Ozark dome is well-suited to studying the effects of river basin dynamics on landscape evolution owing to long-term tectonic stability in a continental interior (Arne et al., 1990; Hudson, 2000), large areas of uniform, gently-dipping sedimentary strata, relatively uniform mean annual precipitation (Fig. 1 and Fig. A.1), and a river network composed primarily of bedrock-floored rivers and mixed alluvial-bedrock beds (Adamski et al., 1995; Keen-Zebert et al., 2017). The region was uplifted in the fore-bulge of the Ouachita Orogen in the late Paleozoic (Hudson, 2000). Offsets on faults in the Ste. Genevieve fault zone indicate that the Ozark dome tilted as a block to the southwest as the Illinois basin subsided (Nelson and Lumm, 1984). Subsidence of the Illinois basin occurred in pulses during the Ouachita Orogeny, with the last subsidence event dated to the Middle Mississippian (Heidlauf et al., 1986). The most recent geologic events recorded in the rock record were the formation of the Mississippi Embayment and the development of the Mississippi drainage system on the eastern side of the Ozark dome in the late Cretaceous (Cox and Van Arsdale, 2002). Although there has been historical seismicity around the dome in the New Madrid seismic zone (Arsdale and Cupples, 2013) and in the Ste. Genevieve fault zone (Yang et al., 2014; Fig. A.2), it is thought that with tectonic loading rates near zero, seismicity in stable continental interiors represents a short-lived release of energy from a prestressed lithosphere (Calais et al., 2016), and hence is unlikely to produce long-lived rock uplift.

Apatite fission track cooling ages from Precambrian granites on the northwest portion of the dome indicate exhumation rates of ~10 m/Ma over the last ~200 Ma (Arne et al., 1990). The modern river network draining the Ozark dome runs primarily perpendicular to the structure contours at the base of Mississippian limestone (Fig. 1), suggesting that the primary structure of the river network formed in response to the Paleozoic deformation field. The Ozark dome and surrounding region remained above sea level during the Mesozoic (Stoeser et al., 2005). The region is also south of the southernmost extent of the Laurentide ice sheet and south of significant glacial isostatic adjustment (Hammond, 2015). Although eustatic sea-level fluctuations and changes in sediment flux occurred during the Quaternary, the frequency of glacial–interglacial cycles is likely too high to affect fluvial profile evolution (Goren, 2016). Given the tectonic and climatic stability of the region, theory predicts that the Ozark dome should have reached a modified erosional steady state in which relief and erosion rate are steady and uniform (Montgomery, 2001).

3. Methods

3.1. Catchment-averaged erosion rates from cosmogenic nuclides

To test whether erosion rates are uniform across the Ozark dome as would be expected in an equilibrium landscape, we measured basin-averaged denudation rates using ^{10}Be in 0.25–0.5 mm quartz grains from recent fluvial deposits in 16 basins that comprised 8 pairs in which each pair share a common divide (Fig. 2a). Samples were collected in streams at drainage areas of ~10 km^2 with paired basins that travel through similar lithologies to minimize effects from heterogeneous lithology. We converted the concentration of ^{10}Be to basin-averaged denudation rates using the CAIRN model (Mudd et al., 2016), which calculates production rates and shielding at each gridcell to account for intra-basin variations in elevation, latitude, slope, aspect, and quartz content. Assuming a uniform denudation rate, the CAIRN model then uses Newton iteration to calculate the denudation rate that results in the closest match to the observed basin-averaged cosmogenic nuclide concentration (Mudd et al., 2016). Production rates are based on the time-independent air pressure scaling schemes of Lal and Stone (Lal, 1991; Stone, 2000) and conversion of elevation and latitude to air pressure (Balco et al., 2008). Denudation rates were converted to erosion rates by assuming a uniform density of 2650 kg/m^3. We used a 90 m resolution DEM for these calculations and eliminated gridcells with non-quartz-bearing lithologies. We considered limestone to be the only non-quartz-bearing lithology; although the limestone in this region is chert-bearing, we did not analyze any chert. We considered the Ordovician dolostone of the Ozark dome (Fig. A.1) to be quartz-bearing because sandstone underlies the dolostone in these formations (Stoeser et al., 2005). Samples were prepared and analyzed at PRIME National Laboratory with standard procedures and 07KNSTD was used as the ^{10}Be standard. See Table A.1 for detailed results and basin-averaged data for each sample. Error bars in Fig. 2c reflect total uncertainty whereas error bars in Fig. 2b reflect only internal uncertainty because each pair of basins were close enough in proximity to assume minimal variation in production rate.

3.2. χ maps and χ profiles

Bedrock erosion scales with either unit stream power (Howard, 1994; Siedl and Dietrich, 1992) or shear stress (Howard and Kerby, 1983), with both relationships resulting in the following model for detachment-limited river incision into bedrock in which the elevation of a point along a stream, z, varies with time, t, and distance along the stream, x, according to:

$$\frac{\partial z(x,t)}{\partial t} = U(x,t) - K(x,t)A^m \left| \frac{\partial z(x,t)}{\partial x} \right|^n \quad (1)$$

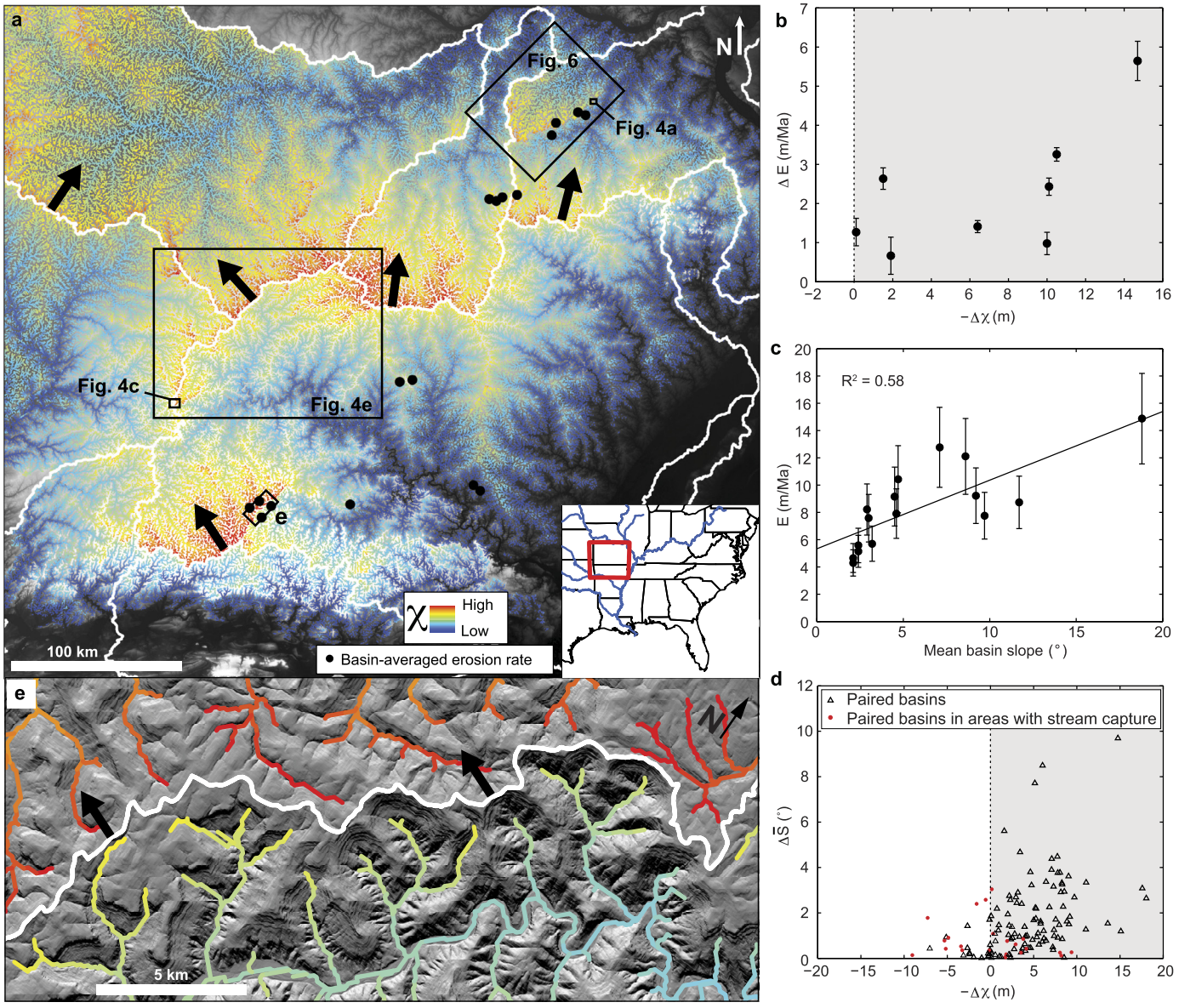

Fig. 2. Drainage basin disequilibrium. **a**, Map of χ across the Ozark dome with black dots showing locations of erosion rate samples. White lines delineate river basin boundaries. Black arrows show predicted divide migration direction. Inset shows location of the study site in central USA. **b**, Plot of the cross-divide difference in basin-averaged erosion rate, ΔE, against the cross-divide difference in mean channel-head χ, $\Delta\chi$. **c**, Plot of basin-averaged erosion rate, E, against mean basin slope. **d**, Plot of cross-divide difference in mean basin slope, ΔS, against $\Delta\chi$. Measurement locations are shown in Fig. A.4. **E**, Hillshade derived from 1 m lidar overlain by a χ map showing an asymmetric divide (large ΔE, ΔS, and $\Delta\chi$). (For a color version of this figure, the reader is referred to the web version of this article.)

where U is rock uplift rate, K is an erosional constant that incorporates rock erodibility, climate, and sediment flux, A is drainage area, which serves as a proxy for discharge, and m and n are empirical constants. Under steady-state conditions, a perfect balance between rock uplift and incision results in time-invariant topography ($\partial z/\partial t = 0$). A solution for the steady-state elevation of a river channel as a function of stream length (x) above base level $z_b(x_b)$ can be obtained via separation of variables:

$$z(x) = z_b + \left(\frac{U}{K A_o^m}\right)^{\frac{1}{n}} \chi \tag{2}$$

where

$$\chi = \int_{x_b}^{x} \left(\frac{A_0}{A(x')}\right)^{\frac{m}{n}} dx' \tag{3}$$

and A_0 is an arbitrary scaling area that gives χ units of length (Perron and Royden, 2013). If U and K are uniform, they can be brought outside the integral as shown in equation (2). χ depends only upon the modern distribution of drainage area, not on topography.

To map the degree of river network disequilibrium on the Ozark dome, we calculated the integral of one over drainage area along the river network, χ. For steady, uniform river incision and rock erodibility, χ scales linearly with elevation (equation (2)) and thus can be used as a proxy for the steady-state elevation of the river network (Willett et al., 2014). Willett et al. (2014) demonstrated that disequilibrium in river basin geometry can be recognized by differences in channel-head χ for channels originating on a common divide.

We calculated flow direction and accumulation using a steepest descent flow algorithm on a 3 arc-second (~90 m) digital elevation model produced from the Shuttle Radar Topography Mission and

downloaded from Open Topography (http://opentopography.org/). We then mapped χ assuming uniform U and K with a concavity, θ, value of 0.45 (Fig. 2). We chose 0.45 because at this value mainstem rivers were relatively straight (Fig. A.2) and χ-plots were pulled above or below the equilibrium line in a direction consistent with independent morphological evidence of area gain or loss (Fig. A.3). We used a scaling area, A_0, of 1 m^2 and a base level of 161 m, the elevation of the confluence of the Osage and Missouri Rivers, which is the lowest possible base level that isolates rivers on the Ozark dome. We defined channel heads using a critical drainage area, A_c, of 0.5 km^2.

3.3. Analysis of cross-divide differences in erosion rate, slope, and χ

To test whether geometric disequilibrium and divide migration direction are correctly inferred from the χ map and profiles, we compared cross-divide differences in χ, $\Delta\chi$, with local metrics of divide motion: cross-divide difference in erosion rates, ΔE, and cross-divide topographic asymmetry, which we measured using cross-divide difference in mean basin slope, ΔS (Fig. 2). Whipple et al. (2017) demonstrated that local metrics of cross-divide differences in erosion rate are better predictors of instantaneous divide motion, whereas cross-divide differences in χ reveal the long-term divide motion that needs to occur to decrease the degree of geometric disequilibrium (Willett et al., 2014). Where erosion rates were measured, we calculated ΔE and $\Delta\chi$ for each pair of basins by subtracting both the erosion rate and the mean channel-head χ of the basin with a lower erosion rate from the basin with a higher erosion rate. To test the correlation between cross-divide difference in χ and topographic asymmetry, we measured $\Delta\chi$ and ΔS in paired basins with drainage area ~10 km^2 along all major divides on the Ozark dome (see Fig. A.4 for locations). To calculate $\Delta\chi$ and ΔS, we subtracted both the mean channel-head χ and mean basin slope of the basin with lower slope from the basin with higher slope. Locally lower χ should indicate a steeper basin, such that where χ correctly predicts topographic asymmetry a negative cross-divide $\Delta\chi$ should correspond to a positive cross-divide ΔS. We used cross-divide difference in mean basin slope as a measure of instantaneous divide migration, although using cross-divide k_{sn} would have produced a similar result (Fig. A.1).

3.4. Estimates of timescales of fluvial profile adjustment and basin geometric adjustment

Whipple et al. (2017) proposed that two timescales are important for understanding landscape evolution under the condition of mobile divides: 1) the fluvial profile response time, defined as the timescale for a fluvial profile to return to an equilibrium form following a drainage area change perturbation; 2) the divide migration timescale, defined as the timescale for basin geometry to reach to an equilibrium shape following some external forcing that perturbs basin geometry. To compare these two timescales for channels on the Ozark dome, we calculated fluvial response times numerically and analytically and estimated the divide migration timescale for a simple divide migration scenario.

To estimate the erodibility, K, which is needed to calculate the fluvial profile response time, we used the channel steepness of quasi-equilibrium channel profiles. χ scales with channel elevation according to the channel steepness, $k_{sn} = (\frac{U}{KA_o^m})^{1/n}$ (Perron and Royden, 2013). Using this equation and assuming $n = 1$, we calculated the erodibility coefficient, K, for the mainstems of the Gasconade and White Rivers (the largest rivers draining the north and south sides of the dome, respectively) from the slopes of the χ-elevation profiles (profiles 2 and 14 in Fig. A.2) and by assuming uplift is equal to the average erosion rate we measured for the dome, $U = 8$ m/Ma. We used a concavity of $\theta = 0.45$ as described in section 3.2 (Fig. A.3). Estimated values for K are 3.1e–6 and 6.7e–7 $m^{0.1}$/yr for the Gasconade and White Rivers, respectively.

Assuming uniform U, $n = 1$, removing A_0, and including K in the integral for χ gives χ units of time, which represents the fluvial response time, τ (Whipple and Tucker, 1999; Goren et al., 2014):

$$\tau = \int_{x_b}^{x} \frac{1}{K(x')} \left(\frac{1}{A(x')} \right)^m dx' \tag{4}$$

Using the values for K estimated for the Gasconade and the Meramec Rivers, $m = 0.45$, and numerically integrating equation (4) using a 90 DEM, we calculated fluvial response time for rivers draining the Ozark dome.

3.4.1. Analytical method for calculating fluvial response time to step changes in drainage area

Changes in drainage area are necessarily accompanied by changes in channel length and basin shape. If we assume drainage area change occurs via divide migration along the entire perimeter of the basin such that geometric similarity is maintained, K is uniform, $n = 1$, and $hm \neq 1$, the response time to a change in drainage area T_{dA} can be found analytically by substituting Hack's Law for drainage area in equation (4) and evaluating the integral from the fluvial channel head at a distance x_c from the drainage divide to base level:

$$T_{dA} = \beta_f / K \tag{5}$$

where $\beta_f = k_a^{-m}(1 - hm)^{-1}(L_f^{1-hm} - x_c^{1-hm})$ is a geometric parameter for the new, post divide migration basin geometry, h is the inverse Hack exponent, k_a is the inverse Hack coefficient, and L_f is the streamwise length of the basin post divide migration. This can be thought of as a minimum fluvial response time as it assumes divides move instantaneously around the full perimeter of the basin in order to maintain a geometry consistent with Hack's Law. This is a limited expression of the area change feedback (Willett et al., 2014) in that basin widening is included as a response to basin lengthening but there is no additional basin lengthening in response to basin widening. Equation (5) differs from that presented in Whipple et al. (2017) in that they neglected changes in channel length when increasing drainage area.

To estimate values of the geometric factor, β, we fit a power function to distance-drainage area data for the White River and the Gasconade River to obtain an inverse Hack exponent of 1.75 (1.74 and 1.76 for the White and the Gasconade Rivers, respectively) and an inverse Hack coefficient of 0.85 (0.80 and 0.93) with R^2 values of 0.98 for the model fits for both rivers. To calculate fluvial response times using equation (5), we used the average length of the dome from the structural axis to the Mississippi Embayment (150 km) for L_f, a critical hillslope length that defines the channel heads, x_c, of 300 m, and both estimated values for K (for the White River and the Gasconade River) discussed above.

3.4.2. Divide migration rates and timescale

To estimate the timescale for river basins to reach geometric equilibrium, τ_{dm}, we calculated divide migration rates for a range of cross-divide erosion differences and slope angles characteristic of divides between asymmetric victim basins and their aggressors on the Ozark dome, such as the Bourbeuse River basin and the Meramec River basin (Fig. 6). For simplicity, we assume that the degree of disequilibrium between adjoining basins is changing slowly such that the divide geometry and cross-divide difference in erosion rate are approximately constant in time. There are, however, scenarios in which the degree of disequilibrium can increase

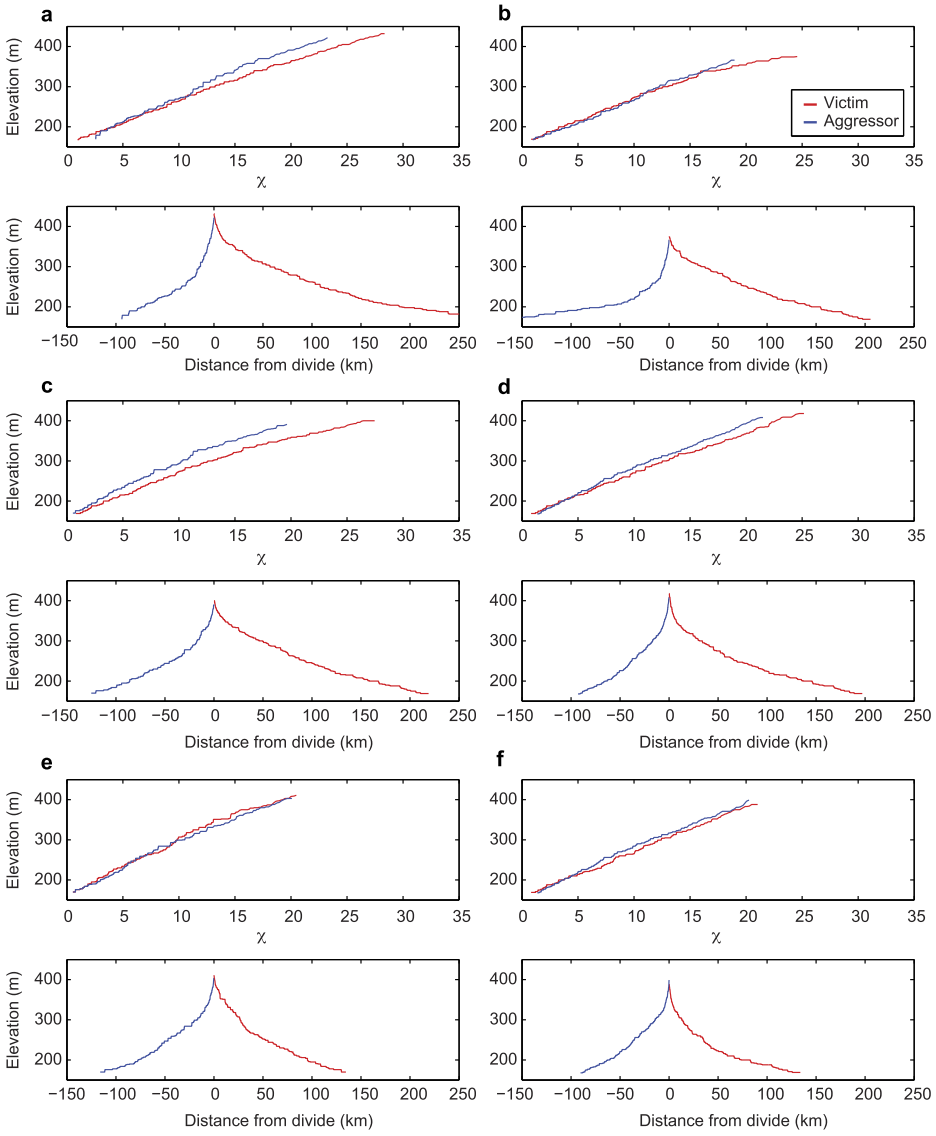

Fig. 3. Cross-divide profiles. A–f, χ-plots (top) and longitudinal profiles (bottom) of paired basins with drainage divides ranging from asymmetric (**a**) to symmetric (**f**). These profiles reflect only the fluvial network. Hillslopes in the region typically comprise <3% of the total relief shown and thus are not be visible at the scale shown. Locations where profiles were taken are shown in Fig. A.4. (For a color version of this figure, the reader is referred to the web version of this article.)

or decrease with time such that cross-divide differences in erosion rate can also increase (Willett et al., 2014) or decrease with time (Whipple et al., 2017). For a drainage divide with planar, time-invariant slopes, it follows that the rate of divide migration is given by:

$$\frac{dx_d}{dt} = \frac{\dot{E}_\alpha - \dot{E}_\beta}{\tan\alpha + \tan\beta} \tag{6}$$

where $\dot{E}_\alpha$ and $\dot{E}_\beta$ are erosion rates on either side of a divide, α and β are the slope angles on opposite sides of the divide, and x_d is the divide position. To compare the timescale of geometric network adjustment with the timescale of longitudinal profile adjustment, a length scale is necessary to convert divide migration rate to time. We used a divide migration length, L, of 10 km because inspection of Fig. 2 indicates that divide migration distances of that order would bring many divides to approximate equilibrium. The divide migration timescale, τ_{dm}, can then be estimated as:

$$\tau_{dm} = \frac{L}{dx_d/dt} \tag{7}$$

4. Results and discussion

4.1. Erosion rates on the Ozark dome

Erosion rates on the Ozark dome range from ~4–15 m/Ma (Table A.1), with a mean of 8 m/Ma, which is similar to the exhumation rate over the last 200 million years (Arne et al., 1990) and similar to or lower than other postorogenic landscapes (Portenga and Bierman, 2011), including the Blue Ridge province of the Appalachian Mountains (Duxbury et al., 2015; Matmon et al., 2003), numerous locations in Australia (Heimsath et al., 2010), and the Cape Mountains of South Africa (Scharf et al., 2013). On the Ozark dome, similarity between erosion rates derived from ^{10}Be, averaged over the last ~100 Ka, and exhumation rates averaged over the last ~200 Ma (Arne et al., 1990) suggests an equilibrium landscape. However, variability exists locally between small contiguous basins (Fig. 2b) by up to a factor of two (Table A.1). This local variability in erosion rates indicates disequilibrium and that the divides separating these basins are actively migrating as cross-divide differences in erosion rates are ultimately what moves divides (Gilbert, 1877; Mudd and Furbish, 2005).

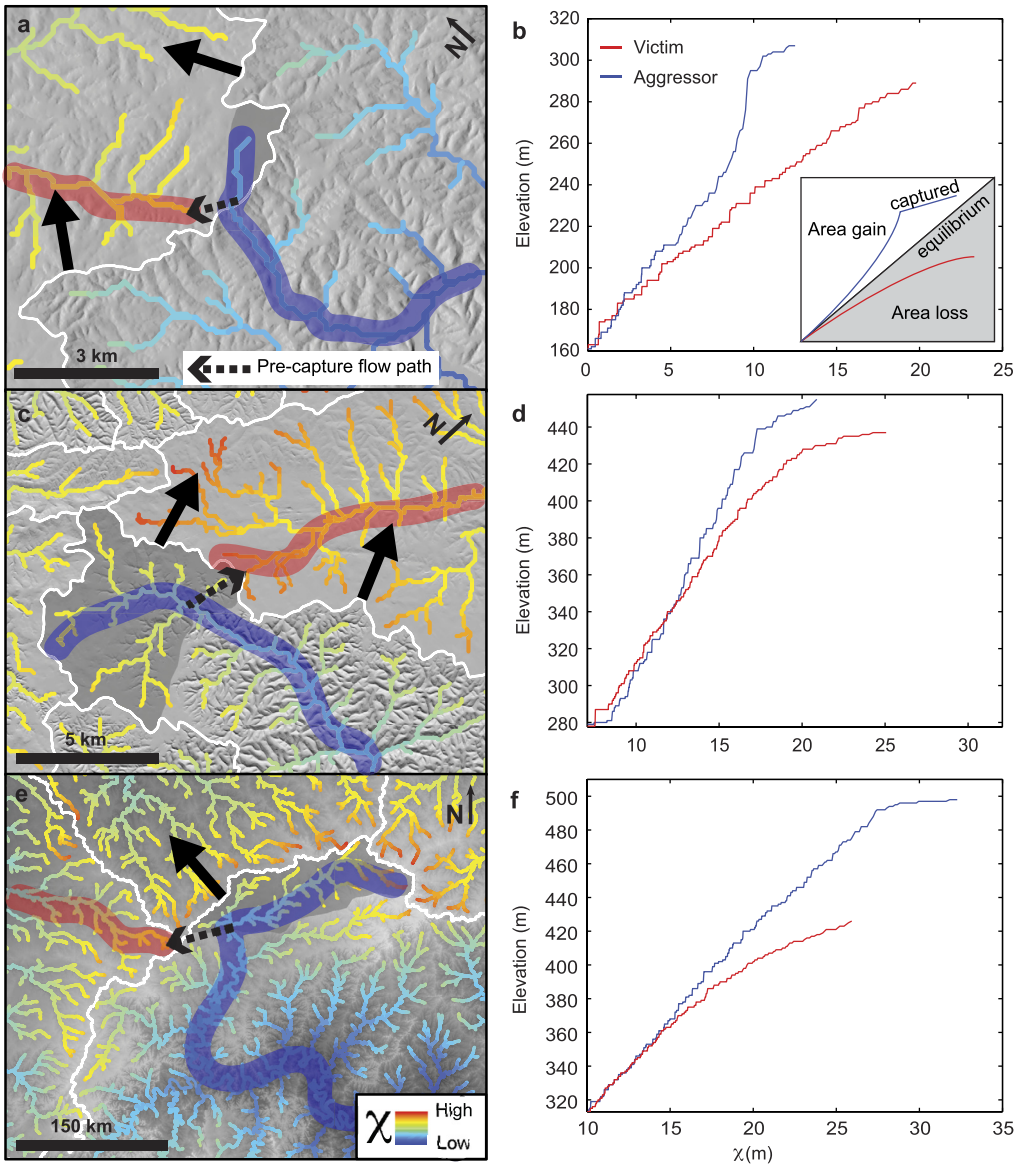

Fig. 4. Evidence of stream capture across scales. (Left) Hillshades overlain by χ maps. White lines show river basin boundaries, solid arrows indicate predicted divide migration direction, arrows with a dashed stem indicate inferred pre-capture drainage direction, and dark grey areas delineate inferred captured drainage area. (Right) χ-plots for the corresponding victims (red) and aggressors (blue). **a**, **b**, 1 km^2 capture of the Bourbeuse River by the Meramec River. **c**, **d**, 30 km^2 capture of Flat Creek by the White River. **e**, **f**, 1000 km^2 capture of the Arkansas River by the White River. Inset in **b** shows the characteristic signature of recent drainage area gain via stream capture in a χ-plot. See Fig. 2 for capture locations. (For a color version of this figure, the reader is referred to the web version of this article.)

4.2. Disequilibrium in river basin geometry drives persistent divide migration on the Ozark dome

The χ map of the Ozark dome (Fig. 2a) reveals large differences in χ across many of the main divides, suggesting that the river network draining the Ozark dome is not in geometric equilibrium and that the river network must reorganize through divide migration and stream capture to attain a stable basin geometry. Changes that perturb a basin away from steady-state can be recognized by deviations from linearity in χ-plots (Willett et al., 2014). χ profiles of the rivers draining the Ozark dome are nearly linear and of similar steepness (Fig. A.2). However, χ profiles on the Ozark dome deviate from linearity systematically and in a manner consistent with drainage area exchange predicted by cross-divide differences in channel-head χ (Fig. 3 and Fig. 4). Thus, we argue that the rivers on the Ozark dome are in a state of quasi-equilibrium, defined as river basins in which the time since the last major perturbation to boundary conditions exceeds one fluvial response time such that there is an approximate balance between rock uplift and erosion, but that they have not reached a perfect steady state because the basin geometry is still out of equilibrium and drainage divides are still mobile.

In the eight paired basins in which we measured erosion rates, the cross-divide difference in erosion rate indicates the divide is migrating in a direction consistent with differences in the channel network geometry as represented by χ (Fig. 2b). Similar to observations made elsewhere (DiBiase et al., 2010; Portenga and Bierman, 2011), erosion rates on the Ozark dome scale with mean basin slope (Fig. 2c) and fluvial steepness, k_{sn} (Fig. A.1), confirming that both are proxies for erosion rate and hence are good local metrics for divide motion. Cross-divide difference in mean basin slope, ΔS, suggests the divides are migrating in a direction consistent with $\Delta\chi$ in paired basins except in cases where the channels have not reached a quasi-equilibrium state owing to recent perturbations such as stream capture (Fig. 2d). In paired basins where recent perturbations have occurred, long-term divide mo-

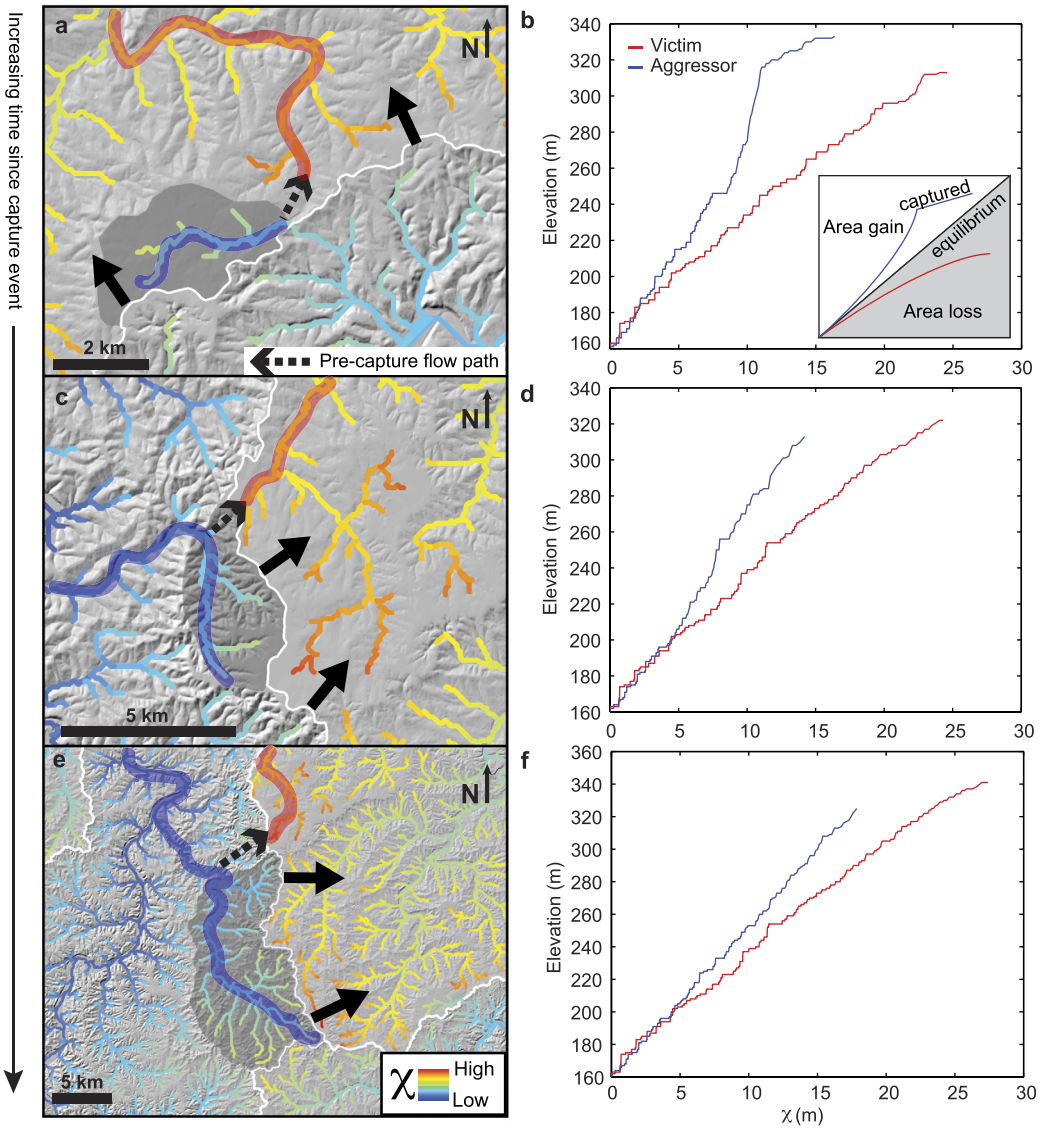

Fig. 5. Stream captures in different stages of equilibration on divides of the Bourbeuse River basin. (Left) Hillshades overlain by χ maps. White lines show drainage divides, arrows indicate the predicted divide migration direction, and dark grey areas delineate captured drainage area inferred from anomalous topology. (Right) χ-plots for the corresponding victims (red) and aggressors (blue). Inset in **b** shows the characteristic signature of recent capture in χ-plots. River basins shown highlight the transient nature of river incision following stream capture with topography in the captured basin that ranges from unadjusted to the new base level (**a**) to nearly adjusted to the new base level (**e**). See Fig. A.4 for capture locations. (For a color version of this figure, the reader is referred to the web version of this article.)

tion is dictated by $\Delta\chi$, which may or may not be consistent with predictions of divide motion based on local metrics (Fig. 2d). Additionally, correlation between cross-divide difference in channel-head χ and divide asymmetry is evident both in hillshade images (e.g. Fig. 2e) and in comparisons between χ-plots and their corresponding longitudinal profiles (Fig. 3). Under quasi-equilibrium conditions, cross-divide difference in channel-head χ correlates with cross-divide differences in k_{sn}, mean basin slope, and erosion rate and thus, in quasi-equilibrium river basins, all four metrics are measures of divide motion. In total, the metrics analyzed indicate the Ozark dome has not reached a steady state because of disequilibrium in river basin geometry, which implies that time to reach steady-state could exceed 100 Ma.

4.3. Persistent drainage area exchange generates discrete, transient geomorphic events

Despite quasi-equilibrium conditions on the Ozark dome, persistent drainage area exchange has generated discrete, transient geomorphic events such as stream capture and the formation of elevated, low-relief surfaces through area-loss feedback. Stream captures change channel network topology and cause transient perturbations to sediment flux and erosion rates (Goren et al., 2014). With evidence in the form of unadjusted topography in the captured reach, anomalous network topology, and characteristic capture signatures in χ-plots, examples of stream captures on the Ozark dome show that capture has occurred across scales, with the inferred captured drainage area ranging from 1–1000 km^2 (Fig. 4). As topography adjusts to a new base level following stream capture, the geomorphic evidence and the characteristic signature in the χ-plot diminish. Different stages of adjustment in stream captures on the same divide illustrate that divide migration has been persistent (Fig. 5).

When sustained for tens to hundreds of millions of years, even small cross-divide differences in erosion rate generated by geometric disequilibrium can give rise to elevated, low-relief surfaces. Basins that lose drainage area and experience a concomitant decrease in erosional power may undergo positive area-loss feedback

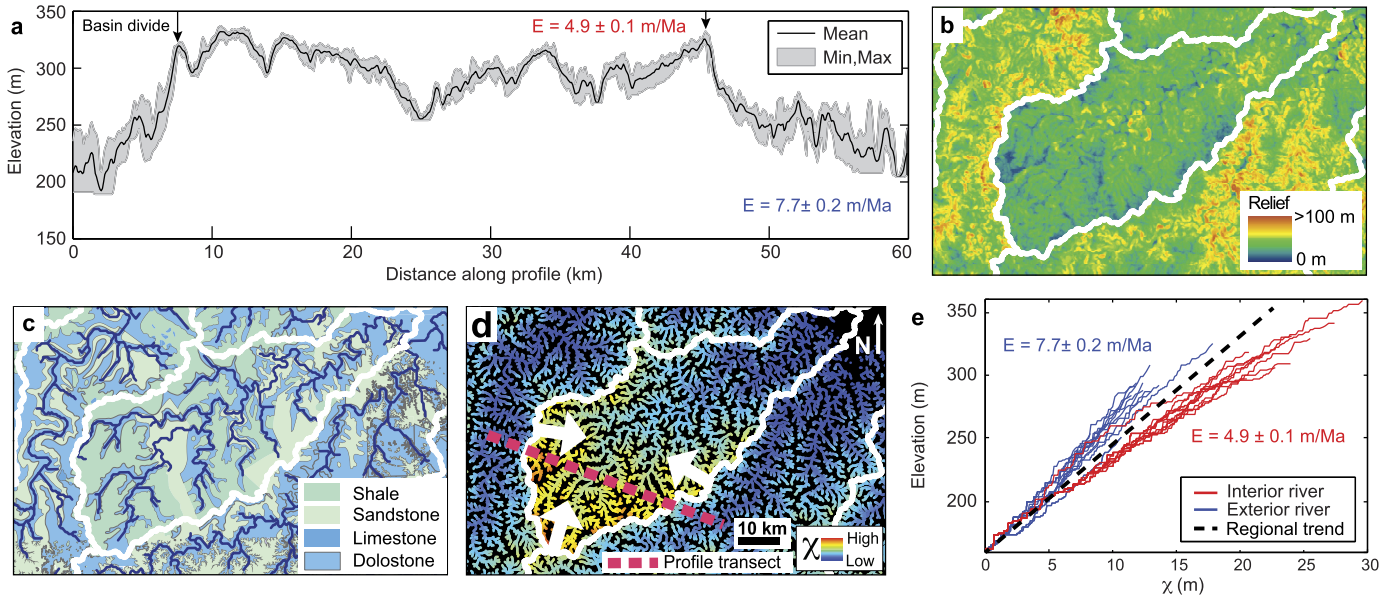

Fig. 6. Persistent, nonuniform erosion rates create elevated, low-relief surfaces. **a**, 1 km wide swath profile across the Bourbeuse River basin from west to east (profile location shown by pink dashed line in **d**). **b**, Map of relief calculated at each gridcell by subtracting the minimum elevation from the maximum elevation within a 500 m moving window showing that the locally low relief is contained within the Bourbeuse River basin. **c**, Geologic map showing that much of the Bourbeuse River Basin is not capped by a resistant lithology, but rather by relatively erodible shale. **d**, χ map centered on the Bourbeuse River basin. White lines show river basin boundaries and arrows indicate the predicted divide migration direction. Pink dashed line shows the location of swath profile shown in **a**. **e**, χ-plot of paired basins, tributaries to either the Bourbeuse River (red interior rivers) or the Meramec or Gasconade Rivers (blue exterior rivers). (For a color version of this figure, the reader is referred to the web version of this article.)

whereby reduced erosion rates lead to a relative increase in elevation and increased susceptibility to further drainage area loss, thus preventing the basins from reaching geometric equilibrium (Willett et al., 2014; Yang et al., 2015). When the area-loss feedback is sustained over time, victim basins will increase in elevation while simultaneously decreasing in relief because of the local reduction in erosion rate combined with loss of drainage area on the perimeter of the basin (Willett, 2017).

An example of an elevated, low-relief surface that may have formed through the area-loss feedback is the Bourbeuse River basin, which stands >100 m higher than the surrounding terrain and has approximately half of the relief within the basin as compared to the surrounding terrain (Figs. 6a, b). While elevated, low-relief surfaces can form because of resistant caprock, the surface formation in the Bourbeuse is shale that is more erodible than other rock types in the basin (Fig. 6c, Fig. A.1). The χ map indicates the Bourbeuse River should lose area along all divides to attain equilibrium (Fig. 6d), and rivers draining the interior of the basin have χ-plots characteristic of drainage area loss whereas rivers draining adjacent basins have χ-plots characteristic of drainage area gain (Fig. 6e). Comparison of the mean erosion rate of two streams draining the interior of the basin (4.9 ± 0.1 m/Ma) with the mean of the cross-divide streams draining adjacent basins (7.7 ± 0.2 m/Ma) confirms an erosion difference between the Bourbeuse River basin and its neighbors, supporting the conclusion of drainage area loss (Figs. 6a, e). If this erosion difference were maintained for 35 Ma, differential erosion could generate the 100 m of relief observed between the Bourbeuse River basin and the surrounding area. Similar surfaces occur across much of the elevation range of the dome (Fig. A.5). They vary in relief and are bounded by drainage divides except in areas where stream capture has moved the divide towards the basin interior, indicating that they are not preserved patches of a former equilibrium landscape (Whipple et al., 2016; Yang et al., 2015). Thus, we argue that multiple elevated, low-relief surfaces on the Ozark dome are not relict uplifted surfaces, but rather have formed *in situ* as a result of long lived area exchange between river basins (Yang et al., 2015).

4.4. Long timescales for planform adjustment of river basin geometry in landscapes with slowly moving drainage divides

For landscapes to achieve steady-state, both channel longitudinal profiles and the planform geometry of the fluvial network must reach equilibrium (Willett et al., 2014; Goren et al., 2014; Whipple, 2001). The time to steady state is set by the sum of these response times. We calculated response time for these two forms of adjustment. Both numerical (Fig. A.6) and analytical (Fig. 7a) calculations of fluvial profile response time on the Ozark dome yield estimates of tens of millions of years, whereas estimates of planform geometric network adjustment via divide migration are of the order of hundreds of millions of years (Fig. 7b). Fluvial response times for $n = 1$ (equation (5)) depend on erodibility and basin geometry and do not change significantly for typical magnitudes of area exchange (Fig. 7a). The timescale of divide migration, however, varies dramatically across a range of reasonable cross-divide differences in erosion rate (Fig. 7b). Thus, ancient postorogenic landscapes like the Ozark dome, which have small cross-divide differences in erosion rate and slowly moving divides, will have large disparities between the timescales of fluvial profile response and of geometric network adjustment (Fig. 7c), the latter of which can approach billions of years (Fig. 7b).

5. Conclusion

Incision across the Ozark dome may have been initiated by Paleozoic tectonic deformation or channel down-cutting through variably erodible stratigraphy (Forte et al., 2016; Perne et al., 2017) or a combination thereof. Regardless of the external forcing that induced geometric disequilibrium, the complex system response of topologic reorganization and persistent divide migration continues to shape the large-scale morphology of the Ozark dome. We conclude that river basin dynamics in landscapes with slowly

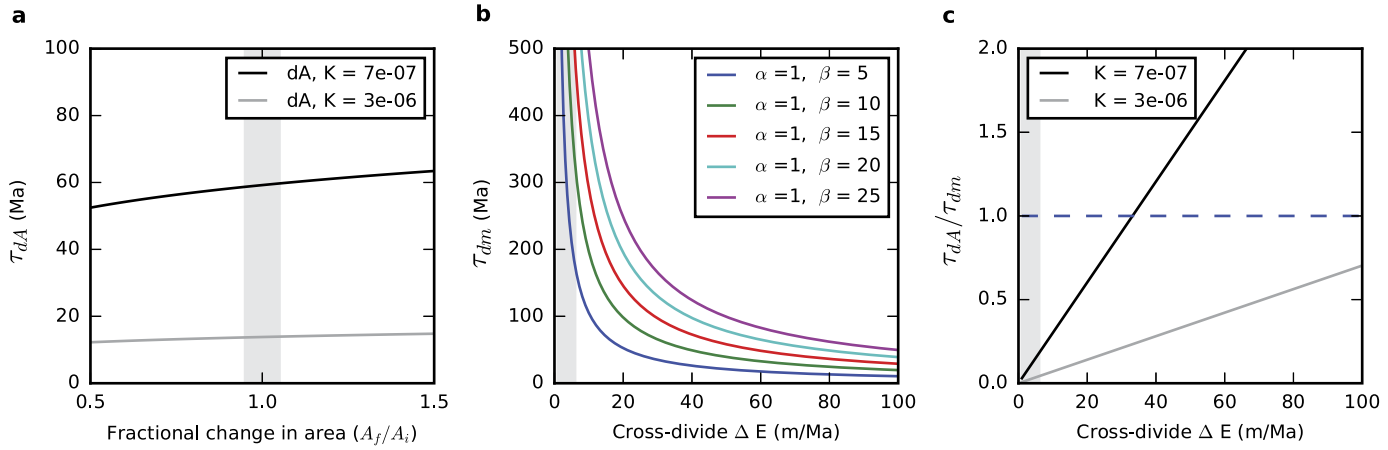

Fig. 7. Comparison of fluvial and geometric response times. a, Plot of fluvial response times to a change in drainage area via divide migration against fractional changes in drainage area (A_f/A_i) for K values estimated from the White and Gasconade Rivers. Range of area change inferred on the Ozark dome (grey bar) can generate cross-divide differences in fluvial response times on the order of 1 Ma, in which basins having gained drainage area and length experience longer response times than before area gain and basins losing drainage area experience shorter response times. **b**, Plot of divide migration timescale against cross-divide difference in erosion rate; calculated using a range of slope angles on opposing sides of the divide (α and β) characteristic of Ozark asymmetric divides (Methods). Erosion rate differences measured in this study are highlighted with the grey bar. **c**, Plot of the ratio of fluvial response time with no area change (from (a) where $A_f/A_i = 1$) to the geometric response time of a divide with hillslope angles of 1 and 10 degrees (green line in (b) against cross-divide difference in erosion rate). Erosion rate differences measured in this study are highlighted with the grey bar.

moving drainage divides can protract time to steady-state to such a degree that postorogenic landscapes may never reach equilibrium. Persistent divide migration maintains a disequilibrium state characterized by nonuniform erosion rates and changing network topology. Thus, although landscapes with slowly moving drainage divides will likely have quasi-equilibrium fluvial longitudinal profiles owing to the discrepancy in timescale between fluvial profile adjustment and divide migration, these landscapes are far from static time-invariant forms.

Acknowledgements

This work was supported by NSF grant EAR-1360572 awarded to Amanda Keen-Zebert, a Geological Society of America J. Hoover Mackin Research Award, and the 2016 University of Nevada Graduate Student Association Research Grant both awarded to Helen W. Beeson. Jack Zunka and Stephen Lancaster contributed one unpublished ^{10}Be concentration to the dataset presented in this study. Darryl Granger and others at the PRIME National Laboratory assisted with sample preparation. We thank Sean Willett for many stimulating discussions during the course of this work and acknowledge anonymous reviews that improved the clarity of the manuscript.

Appendix A. Supplementary material

Supplementary material related to this article can be found online at http://dx.doi.org/10.1016/j.epsl.2017.07.010. These data include six supplemental figures and a table with detailed data for each erosion rate sample as well as a chi map for the Ozark dome and erosion rate data in KML format.

References

Adamski, J.C., Petersen, J.C., Freiwald, D.A., Davis, J.V., 1995. Environmental and hydrologic setting of the Ozark Plateaus study unit, Arkansas, Kansas, Missouri, and Oklahoma. National Water-Quality Assessment Program.

Ahnert, F., 1970. Functional relationships between denudation, relief, and uplift in large, mid-latitude drainage basins. Am. J. Sci. 268, 243–263. http://dx.doi.org/10.2475/ajs.268.3.243.

Arne, D.C., Green, P.F., Duddy, I.R., 1990. Thermochronologic constraints on the timing of Mississippi Valley-type ore formation from apatite fission track analysis. Int. J. Radiat. Appl. Instrum., Part D Nucl. Tracks Radiat. Meas. 17, 319–323.

Arsdale, R.V., Cupples, W., 2013. Late Pliocene and Quaternary deformation of the Reelfoot rift. Geosphere 9, 1819–1831. http://dx.doi.org/10.1130/GES00906.1.

Balco, G., Stone, J.O., Lifton, N.A., Dunai, T.J., 2008. A complete and easily accessible means of calculating surface exposure ages or erosion rates from ^{10}Be and ^{26}Al measurements. Quat. Geochronol. 3, 174–195. http://dx.doi.org/10.1016/j.quageo.2007.12.001.

Calais, E., Camelbeeck, T., Stein, S., Liu, M., Craig, T.J., 2016. A new paradigm for large earthquakes in stable continental plate interiors. Geophys. Res. Lett. 43, 10,621–10,637. http://dx.doi.org/10.1002/2016GL070815.

Cox, R.T., Van Arsdale, R.B., 2002. The Mississippi Embayment, North America: a first order continental structure generated by the Cretaceous superplume mantle event. J. Geodyn. 34, 163–176. http://dx.doi.org/10.1016/S0264-3707(02)00019-4.

DiBiase, R.A., Whipple, K.X., Heimsath, A.M., Ouimet, W.B., 2010. Landscape form and millennial erosion rates in the San Gabriel Mountains, CA. Earth Planet. Sci. Lett. 289, 134–144. http://dx.doi.org/10.1016/j.epsl.2009.10.036.

Dietrich, W.E., Bellugi, D.G., Sklar, L.S., Stock, J.D., Heimsath, A.M., Roering, J.J., 2003. Geomorphic transport laws for predicting landscape form and dynamics. In: Wilcock, P.R., Iverson, R.M. (Eds.), Prediction in Geomorphology. In: Geophysical Monograph Series. American Geophysical, Union, Washington, DC, pp. 103–132.

Duxbury, J., Bierman, P.R., Portenga, E.W., Pavich, M.J., Southworth, S., Freeman, S.P.H.T., 2015. Erosion rates in and around Shenandoah National Park, Virginia, determined using analysis of cosmogenic ^{10}Be. Am. J. Sci. 315, 46–76. http://dx.doi.org/10.2475/01.2015.02.

Forte, A.M., Yanites, B.J., Whipple, K.X., 2016. Complexities of landscape evolution during incision through layered stratigraphy with contrasts in rock strength. Earth Surf. Process. Landf. 41, 1736–1757. http://dx.doi.org/10.1002/esp.3947.

Gilbert, G.K., 1877. Geology of the Henry Mountains, Utah, Geographical and Geological Survey of the Rocky Mountains Region. US Government Printing Office, Washington, DC, US.

Goren, L., 2016. A theoretical model for fluvial channel response time during time-dependent climatic and tectonic forcing and its inverse applications. Geophys. Res. Lett. 43, 10,753–10,763. http://dx.doi.org/10.1002/2016GL070451.

Goren, L., Willett, S.D., Herman, F., Braun, J., 2014. Coupled numerical-analytical approach to landscape evolution modeling. Earth Surf. Process. Landf. 39, 522–545. http://dx.doi.org/10.1002/esp.3514.

Hammond, W., 2015. GPS Imaging of Global Vertical Land Motion for Sea Level Studies. Presented at the 2015 AGU Fall Meeting, Agu.

Hasbargen, L.E., Paola, C., 2000. Landscape instability in an experimental drainage basin. Geology 28, 1067–1070. http://dx.doi.org/10.1130/0091-7613(2000)28<1067:LIIAED>2.0.CO;2.

Heidlauf, D.T., Hsui, A.T., dev Klein, G., 1986. Tectonic subsidence analysis of the Illinois Basin. J. Geol., 779–794.

Heimsath, A.M., Chappell, J., Fifield, K., 2010. Eroding Australia: rates and processes from Bega Valley to Arnhem Land. Geol. Soc. (Lond.) Spec. Publ. 346, 225–241. http://dx.doi.org/10.1144/SP346.12.

Howard, A.D., 1982. Equilibrium and time scales in geomorphology: application to sand-bed alluvial streams. Earth Surf. Process. Landf. 7, 303–325.

Howard, A.D., 1994. A detachment-limited model of drainage basin evolution. Water Resour. Res. 30, 2261–2285. http://dx.doi.org/10.1029/94WR00757.

Howard, A.D., Kerby, G., 1983. Channel changes in badlands. Geol. Soc. Am. Bull. 94, 739–752. http://dx.doi.org/10.1130/0016-7606(1983)94<739:CCIB>2.0.CO;2.

Hudson, M.R., 2000. Coordinated strike-slip and normal faulting in the southern Ozark dome of northern Arkansas: deformation in a late Paleozoic foreland. Geology 28, 511–514.

Keen-Zebert, A.K., Hudson, M., Shepherd, S., Thaler, E., 2017. The effect of lithology on valley width, terrace distribution, and bedload provenance in a tectonically stable catchment with flat-lying stratigraphy. Earth Surf. Process. Landf. http://dx.doi.org/10.1002/esp.4116.

Kirby, E., Whipple, K.X., 2012. Expression of active tectonics in erosional landscapes. J. Struct. Geol. 44, 54–75. http://dx.doi.org/10.1016/j.jsg.2012.07.009.

Kirkby, M., 1971. Hillslope process-response models based on the continuity equation. Inst. Br. Geogr. Spec. Publ. 3, 15–30.

Lal, D., 1991. Cosmic ray labeling of erosion surfaces: in situ nuclide production rates and erosion models. Earth Planet. Sci. Lett. 104, 424–439. http://dx.doi.org/10.1016/0012-821X(91)90220-C.

Matmon, A., Bierman, P.R., Larsen, J., Southworth, S., Pavich, M., Finkel, R., Caffee, M., 2003. Erosion of an Ancient Mountain Range, The Great Smoky Mountains, North Carolina and Tennessee. Am. J. Sci. 303, 817–855. http://dx.doi.org/10.2475/ajs.303.9.817.

Montgomery, D.R., 2001. Slope distributions, threshold hillslopes, and steady-state topography. Am. J. Sci. 301, 432–454.

Mudd, S.M., Furbish, D.J., 2005. Lateral migration of hillcrests in response to channel incision in soil-mantled landscapes. J. Geophys. Res., Earth Surf. 110, F04026. http://dx.doi.org/10.1029/2005JF000313.

Mudd, S.M., Harel, M.-A., Hurst, M.D., Grieve, S.W.D., Marrero, S.M., 2016. The CAIRN method: automated, reproducible calculation of catchment-averaged denudation rates from cosmogenic nuclide concentrations. Earth Surf. Dyn. 4, 655–674. http://dx.doi.org/10.5194/esurf-4-655-2016.

Nelson, W.J., Lumm, D.K., 1984. Structural Geology of Southeastern Illinois and Vicinity (No. NUREG/CR-4036). Illinois State Geological Survey, Champaign, USA.

Pazzaglia, F.J., 2003. Landscape evolution models. In: Developments in Quaternary Sciences. Elsevier, pp. 247–274.

Perne, M., Covington, M.D., Thaler, E.A., Myre, J.M., 2017. Steady state, erosional continuity, and the topography of landscapes developed in layered rocks. Earth Surf. Dyn. 5, 85–100. http://dx.doi.org/10.5194/esurf-5-85-2017.

Perron, J.T., Royden, L., 2013. An integral approach to bedrock river profile analysis. Earth Surf. Process. Landf. 38, 570–576. http://dx.doi.org/10.1002/esp.3302.

Portenga, E.W., Bierman, P.R., 2011. Understanding Earth's eroding surface with ^{10}Be. GSA Today 21, 4–10. http://dx.doi.org/10.1130/G111A.1.

Prince, P.S., Spotila, J.A., Henika, W.S., 2011. Stream capture as driver of transient landscape evolution in a tectonically quiescent setting. Geology 39, 823–826. http://dx.doi.org/10.1130/G32008.1.

Reinhardt, L., Ellis, M.A., 2015. The emergence of topographic steady state in a perpetually dynamic self-organized critical landscape. Water Resour. Res. 51, 4986–5003. http://dx.doi.org/10.1002/2014WR016223.

Scharf, T.E., Codilean, A.T., Wit, M., de Jansen, J.D., Kubik, P.W., 2013. Strong rocks sustain ancient postorogenic topography in southern Africa. Geology 41, 331–334. http://dx.doi.org/10.1130/G33806.1.

Siebenthal, C.E., 1915. Origin of the zinc and lead deposits of the Joplin Region: Missouri, Kansas, and Oklahoma.

Siedl, M.A., Dietrich, W.E., 1992. The problem of channel erosion into bedrock. Catena, Suppl. 23, 101–124.

Stoeser, D.B., Green, G.N., Morath, L.C., Heran, W.D., Wilson, A.B., Moore, D.W., Gosen, B.S.V., 2005. Preliminary integrated geologic map databases for the United States. US Geol. Surv. Open-File Rep. 1351.

Stone, J.O., 2000. Air pressure and cosmogenic isotope production. J. Geophys. Res., Solid Earth 105, 23753–23759. http://dx.doi.org/10.1029/2000JB900181.

Tucker, G.E., Whipple, K.X., 2002. Topographic outcomes predicted by stream erosion models: sensitivity analysis and intermodel comparison. J. Geophys. Res. 107. http://dx.doi.org/10.1029/2001JB000162.

Whipple, K.X., 2001. Fluvial landscape response time: how plausible is steady-state denudation? Am. J. Sci. 301, 313–325. http://dx.doi.org/10.2475/ajs.301.4-5.313.

Whipple, K.X., DiBiase, R.A., Ouimet, W.B., Forte, A.M., 2016. Preservation or piracy: diagnosing low-relief, high-elevation surface formation mechanisms. Geology 45. http://dx.doi.org/10.1130/G38490.1.

Whipple, K.X., Forte, A.M., DiBiase, R.A., Gasparini, N.M., Ouimet, W.B., 2017. Timescales of landscape response to divide migration and drainage capture: implications for the role of divide mobility in landscape evolution. J. Geophys. Res., Earth Surf. 122, 248–273. http://dx.doi.org/10.1002/2016JF003973.

Whipple, K.X., Tucker, G.E., 1999. Dynamics of the stream-power river incision model: implications for height limits of mountain ranges, landscape response timescales, and research needs. J. Geophys. Res., Solid Earth 104, 17661–17674. http://dx.doi.org/10.1029/1999JB900120.

Willett, S.D., 2017. Preservation or piracy: diagnosing low-relief, high-elevation surface formation mechanisms: COMMENT. Geology 45, 91–94. http://dx.doi.org/10.1130/G38929C.1.

Willett, S.D., McCoy, S.W., Perron, J.T., Goren, L., Chen, C.-Y., 2014. Dynamic reorganization of river basins. Science 343, 1248765. http://dx.doi.org/10.1126/science.1248765.

Yang, R., Willett, S.D., Goren, L., 2015. In situ low-relief landscape formation as a result of river network disruption. Nature 520, 526–529. http://dx.doi.org/10.1038/nature14354.

Yang, X., Pavlis, G.L., Hamburger, M.W., Sherrill, E., Gilbert, H., Marshak, S., Rupp, J., Larson, T.H., 2014. Seismicity of the Ste. Genevieve seismic zone based on observations from the EarthScope OIINK flexible array. Seismol. Res. Lett. 85, 1285–1294. http://dx.doi.org/10.1785/0220140079.